DMD Fast Forward. Published on July 9, 2009 as doi:10.1124/dmd.108.024596

Functional Characterization of Low-Prevalence Missense Polymorphisms in the UGT1A9 Gene

Kristine C. Olson, Ryan W. Dellinger, Qing Zhong, Dongxiao Sun, Shantu Amin, Thomas E. Spratt, and Philip Lazarus

Cancer Control and Population Sciences Program (K.C.O., R.W.D., D.S., Q.Z., P.L.), and Chemical Carcinogenesis and Chemoprevention Program (S.A., T.E.S.), Penn State Cancer Institute; Departments of Pharmacology (K.C.O, R.W.D., D.S., Q.Z., S.A., P.L.), Biochemistry and Molecular Biology (T.E.S.), and Public Health Sciences (P.L.), Penn State University College of Medicine, Hershey, PA 17033

Running title: UGT1A9 polymorphisms and homodimerization and activity

Corresponding author: Philip Lazarus, Ph.D., Penn State Cancer Institute, Penn State University College of Medicine, Rm. T3427, MC-CH69, 500 University Drive, Hershey, PA 17033; Fax: (717) 531-0480; Email: plazarus@psu.edu

Number of text pages: 37

Number of tables: 2

Number of figures: 4

Number of references: 39

Number of words in Abstract: 230

Number of words in Introduction: 547

Number of words in Discussion: 1181

Abbreviations: UGT, UDP-glucuronosyltransferase; UDPGA, UDP-glucuronic acid; PAH, polycyclic aromatic hydrocarbon; B[a]P, benzo[a]pyrene; 3-OH-B[a]P, 3-hydroxy-benzo[a]pyrene; 11-OH-DB[a,l]P, 11-hydroxy-dibenzo[a,l]pyrene; 4-MU, 4-methylumbelliferone; 4-ABP, 4-aminobiphenyl; UPLC, Ultra performance liquid chromatography; PCR, polymerase chain reaction; RFLP, restriction fragment length polymorphisms analysis; ER, endoplasmic reticulum; K_m, apparent Michaelis constant; V_{max}, maximum rate; K_i, substrate inhibition constant; K_S, substrate dissociation constant; SNP, single nucleotide polymorphism.

DMD Fast Forward. Published on July 9, 2009 as DOI: 10.1124/dmd.108.024596
This article has not been copyedited and formatted. The final version may differ from this version.

ABSTRACT

The UDP-glucuronosyltransferase (UGT) 1A9 has been shown to play an important role in the detoxification of several carcinogens and clearance of anti-cancer and pain medications. The goal of the present study was to identify novel polymorphisms in UGT1A9 and characterize their effect on glucuronidation activity. The UGT1A9 gene was analyzed by direct sequencing of buccal cell genomic DNA from 90 healthy subjects. In addition to a previously-identified single nucleotide polymorphism (SNP) at codon 33 resulting in an amino acid substitution (Met>Thr), two low-prevalence (<0.02) novel missense SNPs at codons 167 (Val>Ala) and 183 (Cys>Gly) were identified and are present in both Caucasians and African American subjects. Glucuronidation activity assays using HEK293 cell lines over-expressing wild-type or variant UGT1A9 demonstrated that the UGT1A9^{33Thr} and UGT1A9^{183Gly} variants exhibited differential glucuronidation activities as compared to wild-type UGT1A9, but this was substrate-dependent. The UGT1A9^{167Ala} variant exhibited similar levels of activity to wild-type as compared to wild-type for all substrates tested. While the wild-type and UGT1A9^{33Thr} and UGT1A9^{167Ala} variants formed homodimers as determined by Western blot analysis of native polyacrylamide gels, the UGT1A9^{183Gly} variant was incapable of homodimerization. These results suggest that several low-prevalence missense polymorphisms exist for UGT1A9 and that two of these (Met33Thr and Cys183Gly) are functional. These results also suggest that while Cys183 is necessary for UGT1A9 homodimerization, the lack of capacity for UGT1A9 homodimerization is not sufficient to eliminate UGT1A9 activity.

DMD Fast Forward. Published on July 9, 2009 as DOI: 10.1124/dmd.108.024596
This article has not been copyedited and formatted. The final version may differ from this version.

INTRODUCTION

The UDP-glucuronosyltransferase (UGT) superfamily of enzymes catalyzes the glucuronidation of a variety of endogenous compounds such as bilirubin and steroid hormones, as well as xenobiotics such as drugs and environmental carcinogens (Tephly and Burchell, 1990; Owens and Ritter, 1995; Gueraud and Paris, 1998; Ren et al., 2000; Tukey and Strassburg, 2000). The UGTs are membrane-bound proteins that, with the exception of UGT1A10 (Dellinger et al., 2007), reside mainly in the endoplasmic reticulum (ER; Tukey and Strassburg, 2000) and are known to exist as monomeric proteins but are capable of homo- and heterodimerization (Ghosh et al., 2001; Operana and Tukey, 2007). The cysteine residues of UGT1A enzymes are highly conserved in all human family members (Figure 1) as well as in other mammals (Ghosh et al., 2005), but the cysteine residues involved in dimerization and the functional implications of human UGT dimerization have yet to be elucidated.

Based upon structural and amino acid sequence homology, UGTs are classified into several families and subfamilies (Mackenzie et al., 2005). The two major families of the UGTs are the UGT1A and UGT2B families (Mackenzie et al., 2005). While the UGT2B family members are derived from independent genes located in chromosome 4, the entire UGT1A family is derived from a single gene locus in chromosome 2, coding for nine functional proteins that differ only in their amino-terminus as a result of alternate splicing of independent exon 1 regions to a shared carboxy-terminus encoded by exons 2-5 (Owens and Ritter, 1995; Nagar and Remmel, 2006). These independent exon 1 regions are responsible for the wide range of substrate specificity demonstrated by the

UGT1A family of enzymes while the common region coded by exons 2-5 is involved in UDP-glucuronic acid (UDPGA) binding (Figure 1)(Tukey and Strassburg, 2000). Polymorphisms have been previously identified for many of the UGT genes and several recent studies have examined their potential role in carcinogenesis and in risk for several cancer types (Burchell and Hume, 1999; Zheng et al., 2001; Ockenga et al., 2003; Araki et al., 2005).

UGT1A9 has been shown to be one of the most active hepatic UGT against a variety of substrates including several metabolites of the procarcinogen benzo[a]pyrene (B[a]P; Dellinger et al., 2006) and is highly active against SN-38, the major active metabolite of the chemotherapeutic agent irinotecan (Gagne et al., 2002). Furthermore, a single nucleotide polymorphism (SNP) identified in UGT1A9 resulting in a methionine to threonine amino acid substitution at codon 33 (UGT1A9^{33Thr}) demonstrated decreased glucuronidation activity against SN-38 *in vitro* (Villeneuve et al., 2003). This observation suggests that genetic variation in the UGT1A9 enzyme may alter a patient's ability to metabolize irinotecan and could affect therapeutic efficacy and drug resistance. However, the effect of this SNP on the ability of UGT1A9 to glucuronidate carcinogens has not been addressed and could be important in identifying individuals at greater risk for cancer.

In the present study, the goal was to identify novel missense SNPs in the UGT1A9 gene and examine how they could potentially affect UGT1A9 function. In addition to the previously-identified UGT1A9^{33Thr} polymorphism, two low-prevalence missense SNPs were also identified in this study: a valine to alanine substitution at codon 167 (UGT1A9^{167Ala}) and a cysteine to glycine substitution at codon 183

(UGT1A9^{183Gly}). Functional characterization of these SNPs with respect to UGT1A9 activity is described.

MATERIALS AND METHODS

Chemicals and materials. 3-Hydroxy-benzo[a]pyrene (3-OH-B[a]P) was purchased from the National Cancer Institute Chemical Carcinogen Repository (Midwest Research Institute, Kansas City, MO). 4-Aminobiphenyl (4-ABP) was purchased from Toronto Research Chemicals (Toronto, ON, Canada). Benzidine and 4-methylumbelliferone (4-MU) were purchased from Sigma (St. Louis, MO). 11-Hydroxy-dibenzo[a,l]pyrene (11-OH-DB[a,l]P) was obtained from the Penn State College of Medicine (Hershey, PA) Organic Synthesis Core. Alamethicin, UDPGA, and β-glucuronidase were purchased from Sigma (St. Louis, MO) and Dulbecco's Modified Eagle's Medium, fetal bovine serum and Geneticin (G418) were purchased from GIBCO (Carlsbad, CA). The human UGT1A Western blotting kit that includes the anti-UGT1A polyclonal antibody was purchased from Gentest (Woburn, MA) while the anti-β-actin monoclonal antibody was obtained from Sigma.

Study Population. For the identification of UGT1A9 polymorphisms and determination of prevalence in different racial groups, our population included 253 Caucasians, 164 African Americans, and 59 Asians as previously described (Richie et al., 1997; Park et al., 2000; Elahi et al., 2002). The allele and genotype frequencies for polymorphisms in the CYP1A1, CYP2E1, GSTM1, GSTT1, and GSTP1 genes in this population was similar to that observed In a pooled analysis of over 15,000 subjects who served as controls in other case-control studies (Garte et al., 2002). Buccal cell samples were collected from all subjects and used for the analysis of polymorphic

UGT1A9 genotypes. Protocols involving the collection and analysis of buccal cell specimens were approved by the institutional review board at the H. Lee Moffitt Cancer Center and collaborating institutes and were in accordance with assurances filed with and approved by the U.S. Department of Health and Human Services. Informed consent was obtained from all subjects.

DNA Sequencing and PCR-RFLP. DNA sequencing was performed at the Penn State College of Medicine Core Facility. For PCR-RFLP analysis, a 760 bp fragment inclusive of the UGT1A9 exon 1 was amplified from genomic DNA for all samples by PCR following established protocols using the following primer set: UGT1A9 RFLP sense (5'- TTTGTGCTGGTATT TCTC-3'), corresponding to bases -80 to -63 relative to the UGT1A9 translation start site, and the UGT1A9 RFLP antisense (5'-ACCGTTTTTTCAAAAATGCC-3'), corresponding to bases +661 to +680 relative to the translation start site (Genbank accession # NM_021027). For identified polymorphisms, PCR products for all samples were then subjected to RFLP analysis with the appropriate enzyme to determine genotype. The enzymes were HpyCH4*V* for codon 3, NCO*I* for codon 33, Bsb*I* for codon 167, and Nla*III* for codon 183.

Cloning, site-directed mutagenesis and generation of cell lines. The wild-type UGT1A9 cDNA was obtained by RT-PCR from total RNA isolated from normal human liver using oligo (dT) as primer. UGT1A9 cDNA was amplified by PCR using the following primers: UGT1A9 sense (5'-AGTTCTCTGATGGCTTGC-3'), corresponding to bases -9 to +9 relative to the UGT1A9 translation start site, and UGT1A9 antisense (5'-TTTTACCTTATTTCCCACCC-3') corresponding to bases +9 to +28 relative to the

UGT1A9 translation stop site (Genbank accession # NM_021027). PCR products were confirmed by dideoxy sequencing and then cloned into the pcDNA3.1 TOPO mammalian expression plasmid (Invitrogen).

UGT1A9 variants were generated by PCR amplification of the pcDNA3.1/V5-His-TOPO vector containing the wild-type UGT1A9 sequence using site-directed mutagenesis primers specific for individual polymorphic site using the QuikChange kit (Stratagene) according to the manufacturer's protocol. The primers used to generate the UGT1A9^{33Thr} variant were: (5'-GCTACTGGTAGTGCCCA**C**GGATGGGAGCCAC TGG-3') and (5'-CCAGTGGCTCCCATCC**G**TGGGCACTACCAGTAGC-3'), corresponding to bases +81-114 relative to the UGT1A9 translation start site; the primers used to generate the UGT1A9^{167Ala} variant were: (5'-CTCCCTCCCCTCCGT GG**C**CTTCGCCAGGGGAATAC-3') and (5'-GTATTCCCCTGGCGAAG**G**CCACGGA GGGGAGGGAG-3'), corresponding to bases +483-517 relative to the UGT1A9 translation start site; and the primers used to generate the UGT1A9^{183Gly} variant were: (5'-GAAGAAGGTGCACAG**G**GCCCTGCTCCTCTTTCCTA-3') and (5'-TAGGAAA GAGGAGCAGGGC**C**CTGTGCACCTTCTTC-3'), corresponding to bases +532-566 relative to the UGT1A9 translation start site (the polymorphic bases are denoted in bold for all primers). The entire coding region for each generated UGT1A9 variant was confirmed by dideoxy DNA sequencing analysis.

Stable UGT1A9-over-expressing cell lines were generated as previously described (Dellinger et al., 2007; Sun et al., 2007). Briefly, the individual UGT1A9 variants were transfected into HEK293 cells (purchased from ATCC; Rockville, MD) by

electroporation. Stable transfectants that over-expressed the individual UGT1A9 variants were selected by treatment with G418 (Invitrogen).

Cellular Microsomal Preparation. Cell homogenates were prepared by resuspending pelleted cells in Tris-buffered saline (25 mM Tris base, 138 mM NaCl, 2.7 mM KCl; pH 7.4) and subjecting them to 3 rounds of freeze-thaw prior to gentle homogenization. Microsomes were prepared from homogenates by centrifugation at 10,000 g for 20 min at 4^{o}C followed by ultra-centrifugation of the supernatant at 100,000 g for 1 h at 4^{o}C to pellet the microsomal fraction. The pellet was then resuspended in Tris-buffered saline and stored in 100 µl aliquots at -70^{o}C. Total cellular microsomal protein concentrations were determined using the BCA assay from Pierce Biotechnology (Rockford, IL) after protein extraction using standard protocols.

Western blot analysis. SDS-PAGE under reducing and non-reducing conditions was performed essentially as described previously (Chen et al., 1997; Ghosh et al., 2001) with the 2X non-reducing buffer containing 1% SDS, 125 mM Tris-HCl pH 6.8, 20% glycerol, 0.5% bromophenol blue. For reducing conditions β-mercaptoethanol (5% final concentration) was added to the non-reducing sample buffer. All samples were boiled for 5 minutes prior to loading. The protein ladder Precision Plus Dual Color Prestained marker (BioRad) was used to assess the protein sizes. Levels of UGT1A9 protein in UGT1A9-over-expressing cell lines were measured by Western blot analysis using the anti-UGT1A antibody (1:5000 dilution as per the manufacturer's instructions), while housekeeping protein levels were assayed using a 1:5000 dilution of β-actin.

Proteins were detected by chemiluminescence using the SuperSignal West Dura Extended Duration Substrate (Pierce Biotechnology, Inc., Rockford, IL). Secondary antibodies supplied with the Dura ECL kit (anti-rabbit and anti-mouse) were used at 1:3000. Relative UGT1A protein levels were quantified against a known amount of human UGT1A protein (100 ng, supplied in the Western blotting kit provided by Gentest) by densitometric analysis of X-ray film exposures (5 sec – 2 min exposures) of Western blots using a GS-800 densitometer with Quantity One software (Bio-Rad, Hercules, CA). Quantification was made relative to the levels of β-actin observed in each lane. X-ray film bands were always below densitometer saturation levels as indicated by the densitometer software. Relative UGT1A protein levels are reported as the mean of three independent Western blot experiments, with Western blot analysis performed using the same UGT1A9-containing microsomes used for activity assays.

Glucuronidation Assays. The rate of glucuronidation by UGT1A9-over-expressing cell microsomes was determined essentially as previously described (Fang et al., 2002; Wiener et al., 2004; Al-Zoughool and Talaska, 2005; Dellinger et al., 2006; Dellinger et al., 2007). For glucuronidation rate determinations, substrate concentrations, microsomal protein levels and incubation times for individual assays were chosen to maximize levels of detection within a linear range of uptake and were similar to established protocols (Fang et al., 2002; Wiener et al., 2004; Dellinger et al., 2007; Sun et al., 2007). For *O*-glucuronidated substrates, kinetic analysis against 3-OH-B[a]P was performed using UGT1A9-overexpressing cell microsomes (1 μg protein) pre-incubated with alamethicin (50 μg/mg protein) for 10 min on ice. The final

DMD Fast Forward. Published on July 9, 2009 as DOI: 10.1124/dmd.108.024596
This article has not been copyedited and formatted. The final version may differ from this version.

incubation reaction was carried out (100 μL final volume) in 50 mM Tris-HCl (pH 7.5), 10 mM $MgCl_2$, 4 mM UDPGA, and 0.25 - 16 μM 3-OH-BaP at 37^{o}C for 15 min. For kinetic analysis of 11-OH-DB[a,l]P, conditions were the same except that 2 μg of microsomal protein was used and the reaction was carried out for 30 min with a substrate concentration range of 0.08 – 5 μM. For kinetic analysis of 4-MU, 5 μg of microsomal protein was used with a substrate concentration range of 100 – 1200 μM for UGT1A9^{33Thr} and 1 – 64 μM for wild-type UGT1A9, UGT1A9^{167Ala} and UGT1A9^{183Gly}. For *N*-glucuronidated substrates, kinetic analysis of 4-ABP was performed using microsomes (40 μg protein) as described above except that the 4-ABP concentration range was 31 - 4000 μM with an incubation time of 120 min. Reactions with benzidine were performed under the same conditions as 4-ABP except that 100 μg of microsomal protein was used with a substrate concentration range of 250 – 8,000 μM. For all calculations involving these UGT1A9-over-expressing cell microsomes, the V_{max} was normalized to UGT levels in the respective cell line based upon Western blot analysis of protein expression for that line. The chosen substrate concentration ranges encompassed the K_m for all conditions tested. Reactions were terminated by the addition of an equal volume of 100% acetonitrile on ice. The reactions were centrifuged at 16,000 g for 10 minutes at 4^{o}C and the supernatant (200 μL) was analyzed by an ultra performance liquid chromatography (UPLC) system (Acquity, Waters), equipped with a UV detector operated at 310 nm (3-OH-B[a]P), 305 nm (11-OH-DB[a,l]P), 316 nm (4-MU), or 280 nm (4-ABP and benzidine), using an UPLC BEH C18 1.7 μm 2.1 x 100 mm column (Acquity, Waters). For both 3-OH-B[a]P and 11-OH-DB[a,l]P, supernatants were concentrated in a speedvac and subsequently resuspended in 20 μL of a 50/50

water/acetonitrile solution in order to allow for glucuronide detection using low concentration ranges for these substrates. The following gradient conditions were utilized for 4-ABP: 80% buffer A (5 mM ammonium acetate, pH 5.0) for 1 min, followed by a linear gradient up to 70% buffer B (100% acetonitrile) over 2 min at a flow rate of 0.3 mL/min. For benzidine, the same buffers were used, except the percentages were adjusted to 95% buffer A with a linear gradient up to 75% of buffer B. For 4-MU, the same buffers were used, except the percentages were adjusted to 98% buffer A with a linear gradient up to 70% of buffer B and a flow rate of 0.5 mL/min. For 3-OH-B[a]P and 11-OH-DB[a,l]P, buffer A contained 5 mM ammonium acetate (pH 5.0) plus 10% acetonitrile. 3-OH-B[a]P conditions were 89% buffer A with a linear gradient up to 67% buffer B at a flow rate of 0.3 mL/min. 11-OH-DB[a,l]P conditions were 78% buffer A with a linear gradient up to 75% buffer B at a flow rate of 0.5 mL/min. Untransfected HEK293 cells were used as a negative control, and putative glucuronide peaks were confirmed first using β-glucuronidase and then liquid chromatography-mass spectrometry as previously described (Dellinger et al., 2006; Sun et al., 2007). Experiments were always performed in triplicate as independent assays.

Data Analysis. GraphPad Prism 5 software (GraphPad Software Inc., San Diego, CA) was employed to calculate kinetic values. Kinetic constants for glucuronidation of all the substrates were calculated using the Michaelis-Menten equation in equation 1:

$$v = \frac{V_{max}\ [S]}{K_m + [S]} \qquad (1)$$

DMD Fast Forward. Published on July 9, 2009 as DOI: 10.1124/dmd.108.024596
This article has not been copyedited and formatted. The final version may differ from this version.

where *v* is the initial rate of reaction, V_{max} is the maximum velocity, K_m is the Michaelis constant, and [S] is the initial substrate concentration. For visualization as to whether the data were consistent with the simple Michaelis-Menten mechanism, the data were transformed into the linear Eadie-Hofstee plots (where x-axis = *v*/[S] and y-axis = *v*)

For the reaction of 3-OH-B[a]P with wild-type UGT1A9 and UGT1A9^{167Ala} and the reaction of 11-OH-DB[a,l]P with UGT1A9^{183Gly}, the data points were fitted to the substrate inhibition model illustrated in Scheme 1 with equation 2.

Scheme 1. Substrate inhibition

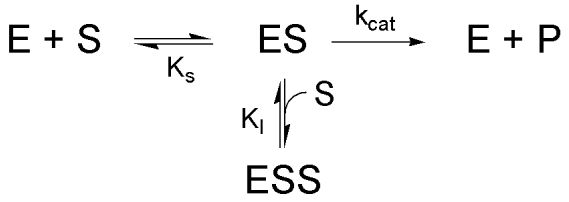

$$v = \frac{V_{max}}{1 + \frac{K_m}{[S]} + \frac{[S]}{K_i}} \qquad (2)$$

where K_i is the substrate inhibition constant.

For the reaction of 3-OH-B[a]P with UGT1A9^{33Thr} and UGT1A9^{183Gly}, the data points were fitted to the substrate activation model in Scheme 2 with equation 3:

Scheme 2. Substrate activation

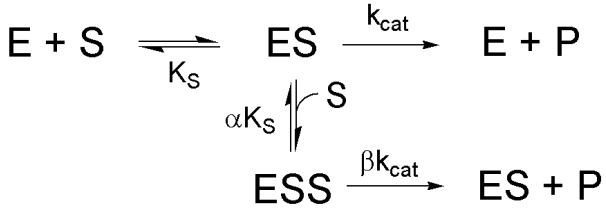

DMD Fast Forward. Published on July 9, 2009 as DOI: 10.1124/dmd.108.024596
This article has not been copyedited and formatted. The final version may differ from this version.

$$\frac{v}{k_{cat}[E]} = \frac{\frac{[S]}{K_S} + \frac{\beta[S]^2}{\alpha K_S^2}}{1 + \frac{[S]}{K_S} + \frac{[S]^2}{\alpha K_S^2}} \quad (3)$$

where K_S is the substrate dissociation constant, αK_S the dissociation constant of the second substrate molecule, and βk_{cat} the rate constant for the product formation from the ESS complex.

The Student's t-test (2-sided) was used for comparing rates and kinetic values of glucuronide formation for the UGT1A9 variants relative to wild-type UGT1A9 against the different substrates examined in this study.

The sequence alignment in Figure 1 was generated by retrieving amino acid sequences for the selected UGTs from the National Center for Biotechnology Information (NCBI) Database and inputting them in FASTA format in the online program ClustalW2 (http://www.ebi.ac.uk/Tools/clustalw2/index.html). Additional annotation to indicate residues or motifs of importance was done by the authors. The structures in Figure 4 were generated by the program ISIS/Draw.

RESULTS

Identification of Novel Missense Polymorphisms in UGT1A9. Informative sequencing information for all UGT1A9 exon 1 sequences was obtained for 90 healthy subjects (43 African Americans and 47 Caucasians). In addition to a previously-identified Met>Thr SNP at codon 33 of the UGT1A9 gene (Villeneuve et al., 2003), two novel missense polymorphisms were identified (Table 1): a T>C at base 500 relative to the UGT1A9 translation start site resulting in a Val>Ala change at UGT1A9 codon 167, and a T>G at base 547 relative to the UGT1A9 translation start site resulting in a Cys>Gly change at UGT1A9 codon 183. Neither of these SNPs was described in public SNP databases including the International HapMap Project. The prevalence of each missense polymorphism was determined by PCR-RFLP analysis of buccal cell DNA from an additional 206 Caucasians, 121 African Americans, and 59 Asians. The prevalence of the UGT1A9^{167Ala} and UGT1A9^{183Gly} variant alleles were both 0.01 in Caucasians, and 0.003 and 0.004, respectively, in African Americans (Table 1). Neither of these missense UGT1A9 variant alleles was found in any of the Asian subjects examined. The prevalence of the UGT1A9^{33Thr} variant was also assessed in our population and was found to be 0.01 in both Caucasians and African-Americans and absent from the Asian population. All of the subjects for which a polymorphism was identified were heterozygous for the polymorphic allele. In addition, a previously-reported UGT1A9 SNP at codon 3 (Villeneuve et al., 2003) was not detected in our populations. None of the variants were linked to each other in any of the subjects examined.

DMD Fast Forward. Published on July 9, 2009 as DOI: 10.1124/dmd.108.024596
This article has not been copyedited and formatted. The final version may differ from this version.

UGT1A9 Variant Activity Analysis. HEK293 cells were stably transfected to overexpress wild-type UGT1A9 (UGT1A9$^{33Met/167Val/183Cys}$). In order to assess whether the missense SNPs in UGT1A9 altered UGT1A9 functional activity, the polymorphic UGT1A9 variants (UGT1A9^{33Thr}, UGT1A9^{167Ala}, and UGT1A9^{183Gly}) were generated by site-directed mutagenesis and individually over-expressed in HEK293 cells since this cell line lacks endogenous UGT expression. Semi-quantitative Western blot analysis was used to determine the expression levels of the individual enzymes (Figure 2). All four cell lines exhibited high levels of UGT1A9 expression. In addition to the band corresponding to the expected UGT1A9 protein at ~50 kDa, a second band of ~100 kDa was observed for wild-type UGT1A9 as well as the UGT1A9^{33Thr} and UGT1A9^{167Ala} variants in native polyacrylamide gels (panel A). This additional band was not observed for the UGT1A9^{183Gly} variant. When UGT1A9-over-expressing HEK293 cell protein was incubated under reducing conditions, the 100 kDa band was no longer detected for any of the UGT1A9 isoforms (panel A). The protein levels of all four UGT1A9 isoforms were determined relative to β-actin (an internal reference for expression) by densitometry under reducing conditions (panel B) and used for normalization of microsomal protein for glucuronidation assays of known substrates of UGT1A9 (described below).

UGT1A9 was previously shown to exhibit the highest *O*-glucuronidating activity of any hepatic UGT against several monohydroxylated B[a]P metabolites including 3-OH-B[a]P (Dellinger et al., 2006). 4-MU is *O*-glucuronidated by many UGT enzymes including UGT1A9 (Mano et al., 2004). In addition to these documented *O*-glucuronidated substrates of UGT1A9, we tested the *O*-glucuronidation activity of UGT1A9 against 11-OH-DB[a,l]P, a metabolite of DB[a,l]P, which is found in cigarette

DMD Fast Forward. Published on July 9, 2009 as DOI: 10.1124/dmd.108.024596
This article has not been copyedited and formatted. The final version may differ from this version.

smoke and is also released in the environment as a result of incomplete combustion of coal and has been proposed as the most potent pro-carcinogen of all polycyclic aromatic hydrocarbons (PAH; Ralston et al., 1995). While UGT1A9 *N*-glucuronidating activity is limited, only two UGTs, 1A4 and 1A9, were shown to *N*-glucuronidate 4-ABP (Al-Zoughool and Talaska, 2006), and UGTs1A4 and 1A9 had the highest levels of *N*-glucuronidating activity against benzidine (Ciotti et al., 1999).

To determine if the polymorphic variants of UGT1A9 produced functional alterations in UGT1A9 *O*- and/or *N*-glucuronidation activity, steady-state kinetic analysis was performed using wild-type and variant UGT1A9-over-expressing HEK293 microsomes in glucuronidation assays with benzidine, 4-ABP, 4-MU, 11-OH-DB[a,l]P, or 3-OH-B[a]P as substrates. The initial rate versus substrate concentration plots are shown in Figure 3. To evaluate whether the initial rate kinetics were consistent with simple Michaelis-Menten kinetics, the data were transformed to the Eadie-Hofstee plots (Supplementary Figure 1). In most cases, the linear Eadie-Hofstee plots indicated that the reactions exhibited Michaelis-Menten kinetics and were fit to equation 1.

The *N*-glucuronidation of benzidine by the three UGT1A9 variants was not significantly different than that observed for wild-type UGT1A9 (Figure 3, Table 2). Glucuronidation of benzidine by human liver microsomes resulted in a much higher glucuronide peak compared to UGT1A9 alone (results not shown), demonstrating that other UGTs (likely UGT1A4) contribute to the *N*-glucuronidation of this compound. *N*-glucuronidation of 4-ABP by wild-type UGT1A9 microsomes was about 30-fold higher as compared to benzidine (Figure 3, Table 2). However, a significantly higher K_m and lower V_{max} was observed for the UGT1A9^{33Thr} variant for 4-ABP, which resulted in

DMD Fast Forward. Published on July 9, 2009 as DOI: 10.1124/dmd.108.024596
This article has not been copyedited and formatted. The final version may differ from this version.

significantly decreased overall glucuronidation (V_{max}/K_m) compared to wild-type UGT1A9. The UGT1A9^{167Ala} variant exhibited a slightly lower K_m with no change in V_{max} or overall glucuronidation efficiency. The UGT1A9^{183Gly} variant exhibited a significantly increased K_m and 2-fold higher V_{max} compared to wild-type UGT1A9, leading to an overall increased glucuronidation efficiency of this mutant versus wild-type.

The *O*-glucuronide substrates were glucuronidated with much higher efficiency by UGT1A9 variants than the two *N*-glucuronidated substrates examined in this study. While the UGT1A9^{33Thr} mutant exhibited large significant increases in K_m and V_{max} and a 25-fold decrease in V_{max}/K_m as compared to wild-type UGT1A9 against 4-MU (Figure 3, Table 2), slight increases in V_{max} and no significant difference in K_m were observed for the UGT1A9^{167Ala} and UGT1A9^{183Gly} variants (Figure 3, Table 2). Glucuronidation of 11-OH-DB[a,l]P was unchanged for the UGT1A9^{33Thr} and UGT1A9^{167Ala} variants, when compared to wild-type UGT1A9. The glucuronidation of 11-OH-DB[a,l]P by UGT1A9^{183Gly} exhibited substrate inhibition as detected by the reduction in *v* at high substrate concentrations (Figure 3) and the decrease in *v* at low *v*/[S] values in the Eadie Hofstee transformed data (Supplemental Figure 1 [SF1]). Thus, these data were fitted to the substrate inhibition kinetic scheme illustrated in Scheme 1 with equation 2. The UGT1A9^{183Gly} variant demonstrated a 3-fold higher K_m, 2-fold higher V_{max}, and a nearly 2-fold decrease in overall enzyme efficiency when compared to wild-type (Table 2). The substrate inhibition constant (K_i) was 6.6 μM, approximately 8-fold higher than the K_m value.

For 3-OH-B[a]P, the wild-type UGT1A9 and the UGT1A9^{167Ala} variant exhibited substrate inhibition kinetics as evidenced by the decreased initial rates at high substrate

concentrations (Figure 3) and curvilinear Eadie-Hofstee plots (SF1). Therefore, the data for both cases were fitted to the substrate inhibition equation (equation 2). The K_m value for UGT1A9^{167Ala} was almost 2-fold higher than the wild-type. V_{max} values for wild-type UGT1A9 and UGT1A9^{167Ala} were virtually the same. The K_is were identical (0.42 μM) for both UGT1A9^{167Ala} and wild-type UGT1A9 (Table 2). The UGT1A9^{33Thr} and UGT1A9^{183Gly} variants exhibited non-Michaelis-Menten kinetics (Figure 3), which was evident after transformation of the data using the Eadie-Hofstee transformation (SF1). As the downward curves of Eadie-Hofstee plots at low v/[S] values suggested substrate inhibition, the upward curve at low v/[S] values for UGT1A9^{33Thr} and UGT1A9^{183Gly} against 3-OH-B[a]P suggested substrate activation. The simplest kinetic scheme that could account for the substrate activation is illustrated in Scheme 2. The rate equation for this scheme is presented in equation 3, where the dissociation constant for the second substrate molecule is αK_S and the ESS complex forms product the rate βk_{cat}. Overall, the kinetic parameters of these fits had large standard deviations from the mean, however this is expected as equation 3 has four variables with a limited amount of data points to fit to a curve. The mean K_S values for UGT1A9^{33Thr} and UGT1A9^{183Gly} (both 0.02 μM) were decreased six-fold from wild-type, however the large standard deviation values made the difference between UGT1A9^{33Thr} and wild-type not statistically different. The large values for α (, α>50) in both cases indicate that the second substrate molecule binds to the complex with less affinity than the first. The V_{max} values for UGT1A9^{33Thr} and UGT1A9^{183Gly} were significantly lower than that observed for wild-type. However, the large β value (β>5 in both cases), indicates that the initial rate of reaction at saturating substrate concentrations would be the same as

wild-type. The overall enzyme efficiency of each of the three variants against 3-OH-B[a]P was unchanged compared to wild-type.

DISCUSSION

The UDP-glucuronosyltransferase (UGT) 1A9 has been shown to play an important role in the detoxification of several carcinogens and clearance of anti-cancer agents and other drugs. In this report, we describe the presence of several low-prevalence SNPs that result in missense changes in the UGT1A9 amino acid sequence. The previously-described SNP resulting in the UGT1A9^{33Thr} variant (Villeneuve et al., 2003), which was also identified in both Caucasians and African Americans in the present study, exhibited changes in *O*-glucuronidation activity against 4-MU and 3-OH-BaP but not 11-OH-DB[a,l]P. Similarly, while a large decrease in activity was observed for this variant against 4-ABP, no difference in activity was observed against benzidine. These results agree with previous studies demonstrating that the UGT1A9^{33Thr} variant exhibited efficient glucuronidation activity against flavopiridol but exhibited a 26-fold decrease in activity against SN-38 (Villeneuve et al., 2003) and significant decreases in glucuronidation activity against mycophenolic acid (Bernard and Guillemette, 2004) and the 4-hydroxylated metabolites of the hormones estradiol and estrone (Thibaudeau et al., 2006). Together, these studies suggest that the glucuronidation efficiency of the UGT1A9^{33Thr} variant appears to be highly substrate-dependent. Interestingly, UGT1A4, which primarily participates in N-glucuronidation, harbors a threonine at the position analogous to Met33 of UGT1A9 (Figure 1). As substrate-dependent glucuronidation efficiency was observed for both *O*- and *N*-glucuronidated substrates in this study, it appears that Met33 is likely not a discriminating residue for *O*- versus *N*-glucuronidation.

Two novel missense SNPs at codons 167 and 183 of the UGT1A9 gene were identified in this study. The UGT1A9^{167Ala} variant exhibited minimal differences in overall glucuronidation activity as compared to wild-type UGT1A9 against all substrates tested in this study. This is consistent with the fact that this polymorphism is relatively conservative, resulting in no changes in charge or polarity at UGT1A9 residue 167. Therefore, such an amino acid change would not be expected to drastically affect enzymatic activity.

Cys183 is a highly-conserved amino acid within the UGT1A family, as it is present in all UGT1A enzymes except UGT1A6 (Figure 1). Previous studies using two-hybrid screening (Ghosh et al., 2001) or fluorescence resonance energy transfer (FRET) analysis (Operana and Tukey, 2007) demonstrated that human UGT1A enzymes may homodimerize. The present study is the first report to identify a cysteine residue that is required for homodimerization of a human UGT. Unlike the strong homodimerization observed for wild-type UGT1A9 or the UGT1A9^{33Thr} and UGT1A9^{167Ala} variants, the UGT1A9^{183Gly} variant specifically exhibited no dimerization potential in the present study, suggesting that the wild-type cysteine at codon 183 is central to UGT1A9 homodimerization. There are thirteen cysteine residues in UGT1A9, with nine conserved among the majority of other human UGT1A enzymes (Figure 1) as well as UGT family members from other mammals (Ghosh et al., 2005). Mutations of each of the eleven cysteine residues in human UGT1A1 was shown to differentially alter *O*-glucuronidation activity against bilirubin, but this report did not address dimerization directly (Ghosh et al., 2005). Similar to the current study, mutation of the cysteine at amino acid residue 186 of the UGT1A1 protein (the analogous cysteine to UGT1A9

codon 183) demonstrated a 2-fold reduction in *O*-glucuronidation activity against bilirubin (Ghosh et al., 2005). Western blot analysis showed that neither the wild-type UGT1A1 nor the Cys186 variant were found to homodimerize, suggesting that the reduced activity of the variant was not attributed to the lack of dimerization through disulfide bonds, but rather the absence of the free thiol groups needed for glucuronidation (Ghosh et al., 2005). In the present study, glucuronidation efficiency of the UGT1A9^{183Gly} mutant was slightly altered, with significantly altered glucuronidation activities against 4-ABP and 11-OH-DB[a,l]P. The glucuronidation efficiency of benzidine, 4-MU, and 3-OH-B[a]P remained relatively unchanged. The abundance of UGT1A9 present in the HEK293 cells may also favor homodimerization of the enzyme, although if this is the case, only 50 percent of UGT1A9 is dimerized as indicated by the Western blot data (Figure 2). Thus, it appears that while a change of the codon 183 cysteine may slightly alter UGT1A9 activity against some substrates, the homodimerization of UGT1A9 is not required for efficient glucuronidation of the substrates we tested.

Little is known about how UGTs select their substrates; however two recent studies identified amino acids that may facilitate unique substrate recognition. In one study, two residues of UGT1A9, Arg42 and Asn152, were identified as contributing to substrate specificity of the enzyme (Fujiwara et al., 2009). The importance of Arg42 and Asn152 was determined using mutational analysis of these amino acids to those analogous found in UGT1A8. In another study, a very low-prevalence polymorphism in the Japanese population, resulting in an aspartic acid to asparagine amino acid change at codon 256 in UGT1A9, differentially affected UGT1A9 glucuronidation of substrates

such as propofol and mycophenolic acid (Takahashi et al., 2008). Consequently, these discriminating residues may be a part of the UGT1A9 substrate binding pocket, and major amino acid changes would affect the glucuronidation ability of the enzyme. In the current study, the UGT1A9^{33Thr} mutant exhibited the most dramatic substrate specific decreases in glucuronidation efficiency. Therefore, it may potentially be part of the substrate binding site and serve as a discriminating residue for substrate selection.

The substrates we tested in the current study are depicted in Figure 4 so that the $–NH_2$ or –OH acceptor group of each substrate is oriented in the same way. In examining the substrates in this manner, it is possible to visualize how the UGT1A9 substrate-binding pocket might accommodate the different structures. Further work with these substrates would be needed to determine the structure-function relationship that is taking place. The glucuronidation of substrates by the UGT family of enzymes is quite variable and is complicated further with the effects of amino acid changes in UGT variants, depending on the severity of change and function of the amino acid. As clearly is the case for 3-OH-B[a]P, the reaction did not follow simple Michaelis-Menten kinetics in the present study. The wild-type UGT1A9 and UGT1A9^{167Ala} followed substrate inhibition kinetics against 3-OH-B[a]P (Scheme 1). UGT1A9^{183Gly} against 11-OH-DB[a,l]P also followed substrate inhibition kinetics. The kinetic analyses for UGT1A9^{33Thr} and UGT1A9^{183Gly} against 3-OH-B[a]P were best fit to Scheme 2, although this does not prove that the reaction occurs via Scheme 2. Complex reaction schemes have been previously observed with UGTs, as Houston and Kenworthy 2000, Galetin et al 2002, Uchaipichat et al 2004, and Uchaipichat et al 2008 have observed kinetics consistent with multiple substrate binding and acceptor sites.

In summary, in addition to a previously-identified SNP at UGT1A9 codon 33 (Villeneuve et al., 2003), two novel low-prevalence missense SNPs were identified in the UGT1A9 gene in this study, both exhibiting relatively modest substrate-specific changes in glucuronidation activity as compared to wild-type UGT19. This is the first report to identify a cysteine that is required for human UGT homodimerization and this result could yield valuable insight into the dynamics of the glucuronidation reaction. While the lack of homodimerization observed for the UGT1A9^{183Gly} variant did not greatly affect UGT1A9 glucuronidation activity against the substrates tested in the present study, a larger evaluation of other substrates may be necessary to examine the overall role of homodimerization on UGT1A9 glucuronidation activities.

ACKNOWLEDGEMENTS

We thank Gang Chen for his helpful discussions and insight, and the Functional Genomics Core Facility and the Molecular Biology Core Facility at the Penn State University College of Medicine for DNA genotyping, DNA sequencing, and usage of densitometric equipment. We also thank the Organic Synthesis Core at the Penn State College of Medicine for synthesizing the 11-OH-DB[a,l]P compound.

REFERENCES

Al-Zoughool M and Talaska G (2005) High-performance liquid chromatography method for determination of N-glucuronidation of 4-aminobiphenyl by mouse, rat, and human liver microsomes. *Anal Biochem* **340:**352-358.

Al-Zoughool M and Talaska G (2006) 4-Aminobiphenyl N-glucuronidation by liver microsomes: optimization of the reaction conditions and characterization of the UDP-glucuronosyltransferase isoforms. *J Appl Toxicol* **26:**524-532.

Araki J, Kobayashi Y, Iwasa M, Urawa N, Gabazza EC, Taguchi O, Kaito M and Adachi Y (2005) Polymorphism of UDP-glucuronosyltransferase 1A7 gene: a possible new risk factor for lung cancer. *Eur J Cancer* **41:**2360-2365.

Bernard O and Guillemette C (2004) The main role of UGT1A9 in the hepatic metabolism of mycophenolic acid and the effects of naturally occurring variants. *Drug Metab Dispos* **32:**775-778.

Burchell B and Hume R (1999) Molecular genetic basis of Gilbert's syndrome. *J Gastroenterol Hepatol* **14:**960-966.

Chen C, Brinkworth R, and Waters MJ (1997) The role of receptor dimerization domain residues in growth hormone signaling. *J Biol Chem* **272**:5133-5140.

Dellinger RW, Chen G, Blevins-Primeau AS, Krzeminski J, Amin S and Lazarus P (2007) Glucuronidation of PhIP and N-OH-PhIP by UDP-glucuronosyltransferase 1A10. *Carcinogenesis* **28:**2412-2418.

Dellinger RW, Fang JL, Chen G, Weinberg R and Lazarus P (2006) Importance of UDP-glucuronosyltransferase 1A10 (UGT1A10) in the detoxification of polycyclic

aromatic hydrocarbons: decreased glucuronidative activity of the UGT1A10139Lys isoform. *Drug Metab Dispos* **34:**943-949.

Elahi A, Zheng Z, Park JY, Eyring K, McCaffrey T and Lazarus P (2002) The human oxoguanine glycosylase 1 (hOGG1) DNA repair enzyme and its association with orolaryngeal cancer risk. *Carcinogenesis* **23:**1229-1234.

Fang JL, Beland FA, Doerge DR, Wiener D, Guillemette C, Marques MM and Lazarus P (2002) Characterization of benzo(a)pyrene-trans-7,8-dihydrodiol glucuronidation by human tissue microsomes and overexpressed UDP-glucuronosyltransferase enzymes. *Cancer Res* **62:**1978-1986.

Fujiwara R, Nakajima M, Yamanaka H, and Yokoi T (2009) Key amino acid residues responsible for the differences in substrate specificity of human UDP-glucuronosyltransferase (UGT)1A9 and UGT1A8. *Drug Metab Dispos* **37:**41-46.

Gagne JF, Montminy V, Belanger P, Journault K, Gaucher G and Guillemette C (2002) Common human UGT1A polymorphisms and the altered metabolism of irinotecan active metabolite 7-ethyl-10-hydroxycamptothecin (SN-38). *Mol Pharmacol* **62:**608-617.

Galetin A, Clarke SE, and Houston JB (2002) Quinidine and haloperidol as modifiers of CYP3A4 activity: multisite kinetic model approach. *Drug Metab Dispos* **30:**1512-1522.

Garte S and 64 others incl. Lazarus P (2002) Metabolic Gene Polymorphism Frequencies in Control Populations. *Cancer Epid. Biomarkers Prev* **10:**1239-1248.

Ghosh SS, Lu Y, Lee SW, Wang X, Guha C, Roy-Chowdhury J and Roy-Chowdhury N (2005) Role of cysteine residues in the function of human UDP glucuronosyltransferase isoform 1A1 (UGT1A1). *Biochem J* **392:**685-692.

Ghosh SS, Sappal BS, Kalpana GV, Lee SW, Chowdhury JR and Chowdhury NR (2001) Homodimerization of human bilirubin-uridine-diphosphoglucuronate glucuronosyltransferase-1 (UGT1A1) and its functional implications. *J Biol Chem* **276:**42108-42115.

Gueraud F and Paris A (1998) Glucuronidation: a dual control. *Gen Pharmacol* **31:**683-688.

Guillemette C, Ritter JK, Auyeung DJ, Kessler FK and Housman DE (2000) Structural heterogeneity at the UDP-glucuronosyltransferase 1 locus: functional consequences of three novel missense mutations in the human UGT1A7 gene. *Pharmacogenetics* **10:**629-644.

Houston JB and Kenworthy KE (2000) In vitro-in vivo scaling of CYP kinetic data not consistend with the classical Michaelis-Menten model. *Drug Metab Dispos* **28:**246-254.

Mackenzie PI, Bock KW, Burchell B, Guillemette C, Ikushiro S, Iyanagi T, Miners JO, Owens IS and Nebert DW (2005) Nomenclature update for the mammalian UDP glycosyltransferase (UGT) gene superfamily. *Pharmacogenet Genomics* **15:**677-685.

Mano Y, Usui T, and Kamimura H (2004) Effects of β-estradiol and propofol on the 4-methylumbelliferone glucuronidation in recombinant human UGT isozymes 1A1, 1A8 and 1A9. *Biopharm Drug Dispos* **25**:339-344.

Nagar S and Remmel RP (2006) Uridine diphosphoglucuronosyltransferase pharmacogenetics and cancer. *Oncogene* **25:**1659-1672.

Ockenga J, Vogel A, Teich N, Keim V, Manns MP and Strassburg CP (2003) UDP glucuronosyltransferase (UGT1A7) gene polymorphisms increase the risk of chronic pancreatitis and pancreatic cancer. *Gastroenterology* **124:**1802-1808.

Operana TN and Tukey RH (2007) Oligomerization of the UDP-glucuronosyltransferase 1A proteins: homo- and heterodimerization analysis by fluorescence resonance energy transfer and co-immunoprecipitation. *J Biol Chem* **282:**4821-4829.

Owens IS and Ritter JK (1995) Gene structure at the human UGT1 locus creates diversity in isozyme structure, substrate specificity, and regulation. *Prog Nucleic Acid Res Mol Biol* **51:**305-338.

Park JY, Muscat J, Schantz S, Stern JC and Lazarus P (2000) Association between GSTM Polymorphisms and Risk for Oral Cancer in African Americans as Compared to Caucasians. *Pharmacogenetics* **10:**123-131.

Ren Q, Murphy SE, Zheng Z and Lazarus P (2000) O-Glucuronidation of the lung carcinogen 4-(methylnitrosamino)-1- (3-pyridyl)-1-butanol (NNAL) by human UDP-glucuronosyltransferases 2B7 and 1A9. *Drug Metab Dispos* **28:**1352-1360.

Ralston SL, Seidel A, Luch A, Platt KL, and Baird WM (1995) Stereoselective activation of dibenzo[*a,l*]pyrene to (-)-*anti*(11*R*,12*S*,13*S*,14*R*)- and (+)-*syn*(11*S*,12*R*,13*S*,14*R*)-11,12-diol-13,14-epoxides which bind extensively to deoxyadenosine residues of DNA in the human mammary carcinoma cell line MCF-7. *Carcinogenesis* **16**:2899-2907.

Richie JP, Jr, Carmella SG, Muscat JE, Scott DG, Akerkar SA and Hecht SS (1997) Differences in the urinary metabolites of the tobacco-specific lung carcinogen 4-(methylnitrosamino)-1-(3-pyridyl)-1-butanone (NNK) in black and white smokers. Cancer Epidemiol. *Biomarkers Prev* **6:**783-790.

Sun D, Sharma AK, Dellinger RW, Blevins-Primeau AS, Balliet RM, Chen G, Boyiri T, Amin S and Lazarus P (2007) Glucuronidation of active tamoxifen metabolites by the human UDP glucuronosyltransferases. *Drug Metab Dispos* **35:**2006-2014.

Takahashi H, Maruo Y, Mori A, Iwai M, Sato H, and Takeuchi Y (2008) Effect of D256N and Y483D on propofol glucuronidation by human uridine 5'-diphosphate glucuronosyltransferase (UGT1A9). *Basic & Clin Pharm & Toxicol* **103:**131-136.

Tephly TR and Burchell B (1990) UDP-glucuronosyltransferases: a family of detoxifying enzymes. *Trends Pharmacol Sci* **11:**276-279.

Thibaudeau J, Lepine J, Tojcic J, Duguay Y, Pelletier G, Plante M, Brisson J, Tetu B, Jacob S, Perusse L, Belanger A, and Guillemette C (2006) Characterization of common UGT1A8, UGT1A9, and UGT2B7 variants with different capacities to inactivate mutagenic 4-hydroxylated metabolites of estradiol and estrone. *Cancer Res* **66**:125-133.

Tukey RH and Strassburg CP (2000) Human UDP-glucuronosyltransferases: metabolism, expression, and disease. *Annu Rev Pharmacol Toxicol* **40:**581-616.

Uchaipichat V, Galetin A, Houston JB, Mackenzie PI, Williams JA, and Miners JO (2008) Kinetic modeling of the interactions between 4-methylumbelliferone, 1-naphthol, and zidovudine glucuronidation by UDP-glucuronosyltransferase 2B7

(UGT2B7) provides evidence for multiple substrate binding and effector sites. *Mol Pharmacol* **74:**1152-1162.

Uchaipichat V, Mackenzie PI, Guo X, Gardner-Stephen D, Galetin A, Houston JB, and Miners JO (2004) Human UDP-glucuronosyltransferases: isoform selectivity and kinetics of 4-methylumbelliferone and 1-naphthol glucuronidation, effects of organic solvents, and inhibition by diclofenac and probenecid. *Drug Metab Dispos* **32:**413-423.

Villeneuve L, Girard H, Fortier LC, Gagne JF and Guillemette C (2003) Novel functional polymorphisms in the UGT1A7 and UGT1A9 glucuronidating enzymes in Caucasian and African-American subjects and their impact on the metabolism of 7-ethyl-10-hydroxycamptothecin and flavopiridol anticancer drugs. *J Pharmacol Exp Ther* **307:**117-128.

Wiener D, Fang JL, Dossett N and Lazarus P (2004) Correlation between UDP-glucuronosyltransferase genotypes and 4-(methylnitrosamino)-1-(3-pyridyl)-1-butanone glucuronidation phenotype in human liver microsomes. *Cancer Res* **64:**1190-1196.

Zheng Z, Park JY, Guillemette C, Schantz SP and Lazarus P (2001) Tobacco carcinogen-detoxifying enzyme UGT1A7 and its association with orolaryngeal cancer risk. *J Natl Cancer Inst* **93:**1411-1418.

DMD Fast Forward. Published on July 9, 2009 as DOI: 10.1124/dmd.108.024596
This article has not been copyedited and formatted. The final version may differ from this version.

FOOTNOTES

K.C.O. and R.W.D. contributed equally to this work.

These studies were supported by Public Health Service (PHS) grants R01-DE13158 (National Institute for Dental and Craniofacial Research) and P01-CA68384 (National Cancer Institute) from the National Institutes of Health, Department of Health and Human Services to P. Lazarus, and formula as well as non-formula funding from the Pennsylvania Department of Health, Health Research Formula and Non-Formula Funding Programs [State of PA, Act 2001-77-part of the PA tobacco settlement legislation to P. Lazarus]

Reprint requests:

Philip Lazarus, Ph.D., Penn State Cancer Institute, Penn State University College of Medicine, Rm. T3427, MC-CH69, 500 University Drive, Hershey, PA 17033; Fax: (717) 531-0480; Email: plazarus@psu.edu

FIGURE LEGENDS

Figure 1. Sequence Alignment of Selected UGTs. The amino acid sequences of full-length UGT1A family members along with UGT2B7 were retrieved from the NCBI protein database and aligned using the online program ClustalW2 (see Materials and Methods). Each of the UGT1A family members contains a unique exon 1 which encodes variable N-terminal amino acids but each UGT1A shares common exons 2-5 coding for the same C-terminal amino acids (shown by the underline); all UGT2B enzymes are derived from unique exons. UGT2B7 is shown as a reference to compare the amino acid similarities and differences with the UGT1A enzymes. Met33, Val167, and Cys183 of UGT1A9 and these amino acids at analogous positions of other UGTs are boxed to show conservation. An asterisk (*) indicates an amino acid fully conserved in all UGT1As as well as UGT2B7 while colon (:) and periods (.) indicate highly conserved and moderately conserved amino acids, respectively, in UGT enzymes. The nine cysteines which are highly conserved in the UGTs are boxed within the UGT sequences. The UGTs are ordered in the alignment by overall conservation of amino acids.

Figure 2. Analysis of UGT1A9 monomer and homodimer expression.
Representative Western blot analysis of the individual UGT1A9-over-expressing cell lines from microsomal protein lysates used in this study. Protein lysate (20 μg) of the indicated UGT1A9 variant over expressing or parental HEK293 cell line was loaded in each lane and screened using a UGT1A-specific antibody (Gentest). **(A)** Western blot

analysis of UGT1A9 using SDS-PAGE. The first 5 lanes were run under non-reducing conditions, while the last four lanes were run under reducing conditions by the addition of β-mercaptoethanol as described in the Materials and Methods; **(B)** Western blot analysis of β–actin. The same blot was stripped and re-probed for β-actin. The relative expression of each UGT1A9 variant was determined by the average of three independent Western blot experiments normalized to β-actin. Wild-type UGT1A9 refers to UGT1A9$^{33Met/167Val/183Cys}$.

Figure 3. Kinetic curves for the *O*- and *N*-glucuronidation of five substrates by wild-type and variant UGT1A9. Glucuronidation assays were performed with microsomes prepared from HEK293 cells overexpressing either wild-type UGT1A9, UGT1A9^{33Thr}, UGT1A9^{167Ala}, or UGT1A9^{183Gly} using benzidine, 4-ABP, 4-MU, 11-OH-DB[a,l]P, or 3-OH-B[a]P as substrate. All data points were fitted to the Michaelis-Menten equation (equation 1) except for the 11-OH-DB[a,l]P reaction with UGT1A9^{183Gly} and the 3-OH-B[a]P reaction with wild-type UGT1A9 and UGT1A9^{167Ala}, which were fitted to the substrate inhibition equation (equation 2). Also, the 3-OH-B[a]P reaction with UGT1A9^{33Thr} and UGT1A9^{183Gly} were fitted to the substrate activation equation (equation 3). The Y-axis represents *v* in units of pmol·min^{-1}·μg^{-1}. The X-axis represents [S] in units of μM.

Figure 4. Structures of the five *O*- and *N*-glucuronidation substrates of UGT1A9. The structures of the three *O*-glucuronidated substrates (4-MU, 3-OH-B[a]P, and 11-OH-DB[a,l]P) and the two *N*-glucuronidated (4-ABP and benzidine) substrates used in

this study are shown. The structures have been oriented according to the $–NH_2$ or –OH acceptor group in which the glucuronic acid will be added.

Supplemental Figure 1. Eadie-Hofstee plots for the *O*- and *N*- glucuronidation of five substrates by wild-type and variant UGT1A9. Kinetic data from Figure 3 were transformed into Eadie-Hofstee plots (where y-axis = *v* and x-axis = *v*/[S]) for benzidine, 4-ABP, 4-MU, 11-OH-DB[a,l]P, and 3-OH-B[a]P as substrates. V is in units of $pmol \cdot min^{-1} \cdot \mu g^{-1}$ and [S] is in units of μM. The lines are the transformation of the lines in Figure 3.

TABLE 1. Allelic prevalence of UGT1A9 polymorphisms in different racial groups.

UGT1A9 variant	SNP	Caucasian (n=250)	African-American (n=153)	Asian (n=59)
codon 33 (Met>Thr)	T98C	0.01	0.01	0
codon 167 (Val>Ala)	T500C	0.01	0.003	0
codon 183 (Cys>Gly)	T547G	0.01	0.004	0

Table 2. Kinetic analysis of glucuronide formation for UGT1A9-overexpressing cell microsomes.[a]

UGT1A9	substrate	K_m or K_s[d] (μM)	V_{max}[b] (pmol·min^{-1}·mg^{-1})	V_{max}/K_m or K_S[b] (μL·min^{-1}·mg^{-1})	Constant values for equation 2[c] or 3[d]
Wild-type	benzidine	2234 ± 439	14 ± 3.4	0.0063 ± 0.0004	
33Thr		1672 ± 336	9.0 ± 1.1	0.0055 ± 0.0005	
167Ala		2295 ± 282	19 ± 2.1	0.0086 ± 0.0017	
183Gly		1971 ± 479	21 ± 4.2	0.011 ± 0.0039	
Wild-type	4-ABP	221 ± 13	48 ± 1.9	0.22 ± 0.02	
33Thr		945 ± 114***	29 ± 1.7***	0.03 ± 0.004***	
167Ala		140 ± 29*	43 ± 9.3	0.31 ± 0.12	
183Gly		280 ± 4.5***	93 ± 19**	0.33 ± 0.06*	
Wild-type	4-MU	5.3 ± 1.3	54 ± 7.3	10 ± 1.5	
33Thr		985 ± 40***	415 ± 3.1***	0.42 ± 0.016***	
167Ala		6.0 ± 1.7	108 ± 14**	19 ± 3.8*	
183Gly		7.1 ± 0.91	87 ± 16*	12 ± 3.8	
Wild-type	11-OH-DB[a,l]P	0.25 ± 0.076	13 ± 3.2	51 ± 9.7	
33Thr		0.32 ± 0.12	19 ± 5.0	59 ± 8.2	
167Ala		0.31 ± 0.15	12 ± 2.2	47 ± 21	
183Gly[c]		0.84 ± 0.09***	26 ± 2.2***	31 ± 2.0*	K_i=6.6 ± 3.2[d]
Wild-type[c]	3-OH-B[a]P	0.12 ± 0.022	40 ± 0.56	337 ± 54	K_i=0.42 ± 0.06[c]
33Thr[d]		0.02 ± 0.083	3.6 ± 10.7**	261 ± 223	α=48.9 ± 171[d] β= 5.87 ± 11.1[d]
167Ala[c]		0.22 ± 0.034*	52 ± 5.3*	246 ± 57	K_i=0.42 ± 0.16[c]
183Gly[d]		0.02 ± 0.050*	7.8 ± 9.9**	525 ± 350	α=78.2 ± 175[d] β=6.72 ± 5.90[d]

[a] Kinetic data are reported as mean ± standard deviation for three independent experiments. K_m represents apparent K_m.
[b] V_{max} values are adjusted per μg of the corresponding UGT1A9 protein as determined by Western blot.
[c] Data were fitted to equation 2 (Materials and Methods), where K_i is the substrate inhibition constant in μM.
[d] Data were fitted to equation 3 (Materials and Methods), where K_S is the substrate dissociation constant, and α and β are constants.
* p<0.05, ** p<0.01, *** p<0.001, relative to wild-type UGT1A9 (UGT1A9$^{33Met/167Val/183Cys}$).

Figure 1

```
UGT1A3     MATGLQVPLPWLATGLLLLLSVQPWAESGKVLVVPIDGSHWLSMREVLRELHARGHQAVVLTPEVNMHIK--EENFFTLTTYAISWTQDEFDRHVLGHTQLYFET--EHFLKKFFRSMAMLNNMSLVYHRSCVEL 131
UGT1A5     MATGLQVPLPQLATGLLLLLSVQPWAESGKVLVVPTDGSHWLSMREALRDLHARGHQVVVLTLEVNMYIK--EENFFTLTTYAISWTQDEFDRLLLGHTQSFFET--EHLLMKFSRRMAIMNNMSLIIHRSCVEL 131
UGT1A4     MARGLQVPLPRLATGLLLLLSVQPWAESGKVLVVPTDGSPWLSMREALRELHARGHQAVVLTPEVNMHIK--EEKFFTLTAYAVPWTQKEFDRVTLGYTQGFFET--EHLLKRYSRSMAIMNNVSLALHRCCVEL 131
UGT1A1     MAVESQGGRP-LVLGLLLCVLGPVVSHAGKILLIPVDGSHWLSMLGAIQQLQQRGHEIVVLAPDASLYIR--DGAFYTLKTYPVPFQREDVKESFVSLGHNVFEN--DSFLQRVIKTYKKIKKDSAMLLSGCSHL 130
UGT1A9     MAC-TGWTSP-LPLCVCLLLTCG-FAEAGKLLVVPMDGSHWFTMRSVVEKLILRGHEVVVVMPEVSWQLG--RSLNCTVKTYSTSYTLEDLDREFKAFAHAQWKAQVRSIYSLLMGSYND---IFDLFFSNCRSL 127
UGT1A8     MAR-TGWTSP-IPLCVSLLLTCG-FAEAGKLLVVPMDGSHWFTMQSVVEKLILRGHEVVVVMPEVSWQLG--KSLNCTVKTYSTSYTLEDLDREFMDFADAQWKAQVRSLFSLFLSSSNG---FFNLFFSHCRSL 127
UGT1A7     MAR-AGWTGL-LPLYVCLLLTCG-FAKAGKLLVVPMDGSHWFTMQSVVEKLILRGHEVVVVMPEVSWQLG--RSLNCTVKTYSTSYTLEDQDREFMVFADARWTAPLRSAFSLLTSSSNG---IFDLFFSNCRSL 127
UGT1A10    MAR-AGWTSP-VPLCVCLLLTCG-FAEAGKLLVVPMDGSHWFTMQSVVEKLILRGHEVVVVMPEVSWQLE--RSLNCTVKTYSTSYTLEDQNREFMVFAHAQWKAQAQSIFSLLMSSSSG---FLDLFFSHCRSL 127
UGT1A6     MAC-LLRSFQRISAGVFFLALWG-MVVGDKLLVVPQDGSHWLSMKDIVEVLSDRGHEIVVVVPEVNLLLK--ESKYYTRKIYPVPYDQEELKNRYQSFGNNHFAE--RSFLTAPQTEYRNNMIVIGLYFINCQSL 129
UGT2B7     --MSVKWTSVILLIQLSFCFSSG---NCGKVLVWAAEYSHWMNIKTILDELIQRGHEVTVLASSASILFDPNNSSALKIEIYPTSLTKTELENFIMQQIKRWSDLPKDTFWLYFSQVQEIMSIFGDITRKFCKDV 130
                  :  : :          .*:*: . : * *:.:   :  *  ***: .*: ...  :         .   *. .    : ..       .                               *  :

UGT1A3     LHNEALIRHLNATSFDVVLTDPVNLCAAVLAKYLSIPTVFFLRNIP-CDLDFKGTQCPNPSSYIPRLLTTNSDHMTFMQRVKNMLYPLALSYICHAF-SAPYASLASELFQREVSVVDILSHASVWLFRGDFVMDY 265
UGT1A5     LHNEALIRHLHATSFDVVLTDPFHLCAAVLAKYLSIPAVFFLRNIP-CDLDFKGTQCPNPSSYIPRLLTTNSDHMTFLQRVKNMLYPLALSYLCHAV-SAPYASLASELFQREVSVVDLVSHASVWLFRGDFVMDY 265
UGT1A4     LHNEALIRHLNATSFDVVLTDPVNLCGAVLAKYLSIPAVFFWRYIP-CDLDFKGTQCPNPSSYIPKLLTTNSDHMTFLQRVKNMLYPLALSYICHTF-SAPYASLASELFQREVSVVDLVSYASVWLFRGDFVMDY 265
UGT1A1     LHNKELMASLAESSFDVMLTDPFLPCSPIVAQYLSLPTVFFLHALP-CSLEFEATQCPNPFSYVPRPLSSHSDHMTFLQRVKNMLIAFSQNFLCDVV-YSPYATLASEFLQREVTVQDLLSSASVWLFRSDFVKDY 264
UGT1A9     FKDKKLVEYLKESSFDAVFLDPFDNCGLIVAKYFSLPSVVFARGIL-CHYLEEGAQCPAPLSYVPRILLGFSDAMTFKERVRNHIMHLEEHLLCHRF-FKNALEIASEILQTPVTEYDLYSHTSIWLLRTDFVLDY 261
UGT1A8     FNDRKLVEYLKESSFDAVFLDPFDACGLIVAKYFSLPSVVFARGIA-CHYLEEGAQCPAPLSYVPRILLGFSDAMTFKERVRNHIMHLEEHLFCQYF-SKNALEIASEILQTPVTAYDLYSHTSIWLLRTDFVLDY 261
UGT1A7     FNDRKLVEYLKESCFDAVFLDPFDACGLIVAKYFSLPSVVFARGIF-CHYLEEGAQCPAPLSYVPRLLLGFSDAMTFKERVWNHIMHLEEHLFCPYF-FKNVLEIASEILQTPVTAYDLYSHTSIWLLRTDFVLEY 261
UGT1A10    FNDRKLVEYLKESSFDAVFLDPFDTCGLIVAKYFSLPSVVFTRGIF-CHHLEEGAQCPAPLSYVPNDLLGFSDAMTFKERVWNHIVHLEDHLFCQYL-FRNALEIASEILQTPVTAYDLYSHTSIWLLRTDFVLDY 261
UGT1A6     LQDRDTLNFFKESKFDALFTDPALPCGVILAEYLGLPSVYLFRGFP-CSLEHTFSRSPDPVSYIPRCYTKFSDHMTFSQRVANFLVNLLEPYLFYCL-FSKYEELASAVLKRDVDIITLYQKVSVWLLRYDFVLEY 263
UGT2B7     VSNKKFMKKVQESRFDVIFADAIFPCSELLAELFNIPFVYSLSFSPGYTFEKHSGGFIFPPSYVPVVMSELTDQMTFMERVKNMIYVLYFDFWFEIFDMKKWDQFYSEVLGRPTTLSETMGKADVWLIRNSWNFQF 266
           . :.  :   .  : **.:: *.    *. ::*: :.:* *                   * **:*      :* *** :** * :  :         .        : * .:   .         ..:**:* .:  ::

UGT1A3     PRPIMPNMVFIGGINCANRKPLSQEFEAYINASGEHGIVVFSLGSMVSEIPEKKAMAIADALGKIPQTVLWRYTGTRPSNLANNTILVKWLPQNDLLGHPMTRAFITHAGSHGVYESICNGVPMVMMPLFGDQMDN 401
UGT1A5     PRPIMPNMVFIGGINCANGKPLSQEFEAYINASGEHGIVVFSLGSMVSEIPEKKAMAIADALGKIPQTVLWRYTGTRPSNLANNTILVKWLPQNDLLGHPMTRAFITHAGSHGVYESICNGVPMVMMPLFGDQMDN 401
UGT1A4     PRPIMPNMVFIGGINCANGKPLSQEFEAYINASGEHGIVVFSLGSMVSEIPEKKAMAIADALGKIPQTVLWRYTGTRPSNLANNTILVKWLPQNDLLGHPMTRAFITHAGSHGVYESICNGVPMVMMPLFGDQMDN 401
UGT1A1     PRPIMPNMVFVGGINCLHQNPLSQEFEAYINASGEHGIVVFSLGSMVSEIPEKKAMAIADALGKIPQTVLWRYTGTRPSNLANNTILVKWLPQNDLLGHPMTRAFITHAGSHGVYESICNGVPMVMMPLFGDQMDN 400
UGT1A9     PKPVMPNMIFIGGINCHQGKPLPMEFEAYINASGEHGIVVFSLGSMVSEIPEKKAMAIADALGKIPQTVLWRYTGTRPSNLANNTILVKWLPQNDLLGHPMTRAFITHAGSHGVYESICNGVPMVMMPLFGDQMDN 397
UGT1A8     PKPVMPNMIFIGGINCHQGKPLPMEFEAYINASGEHGIVVFSLGSMVSEIPEKKAMAIADALGKIPQTVLWRYTGTRPSNLANNTILVKWLPQNDLLGHPMTRAFITHAGSHGVYESICNGVPMVMMPLFGDQMDN 397
UGT1A7     PKPVMPNMIFIGGINCHQGKPVPMEFEAYINASGEHGIVVFSLGSMVSEIPEKKAMAIADALGKIPQTVLWRYTGTRPSNLANNTILVKWLPQNDLLGHPMTRAFITHAGSHGVYESICNGVPMVMMPLFGDQMDN 397
UGT1A10    PKPVMPNMIFIGGINCHQGKPLPMEFEAYINASGEHGIVVFSLGSMVSEIPEKKAMAIADALGKIPQTVLWRYTGTRPSNLANNTILVKWLPQNDLLGHPMTRAFITHAGSHGVYESICNGVPMVMMPLFGDQMDN 397
UGT1A6     PRPVMPNMVFIGGINCKKRKDLSQEFEAYINASGEHGIVVFSLGSMVSEIPEKKAMAIADALGKIPQTVLWRYTGTRPSNLANNTILVKWLPQNDLLGHPMTRAFITHAGSHGVYESICNGVPMVMMPLFGDQMDN 399
UGT2B7     PYPLLPNVDFVGGLHCKPAKPLPKEMEDFVQSSGENGVVVFSLGSMVSNMTEERANVIASALAQIPQKVLWRFDGNKPDTLGLNTRLYKWIPQNDLLGHPKTRAFITHGGANGIYEAIYHGIPMVGIPLFADQPDN 402
           * *::**: *:**::*   : :. *:* ::::***:*:**********::.*::* .**.**.:***.****: *.:*..*. ** * **:********* *******.*::*:**:* :*:*** :***.** **

UGT1A3     AKRMETKGAGVTLNVLEMTSEDLENALKAVINDKSYKENIMRLSSLHKDRPVEPLDLAVFWVEFVMRHKGAPHLRPAAHDLTWYQYHSLDVIGFLLAVVLTVAFITFKCCAYGYRKCLGKKGRVKKAHKSKTH 534
UGT1A5     AKRMETKGAGVTLNVLEMTSEDLENALKAVINDKSYKENIMRLSSLHKDRPVEPLDLAVFWVEFVMRHKGAPHLRPAAHDLTWYQYHSLDVIGFLLAVVLTVAFITFKCCAYGYRKCLGKKGRVKKAHKSKTH 534
UGT1A4     AKRMETKGAGVTLNVLEMTSEDLENALKAVINDKSYKENIMRLSSLHKDRPVEPLDLAVFWVEFVMRHKGAPHLRPAAHDLTWYQYHSLDVIGFLLAVVLTVAFITFKCCAYGYRKCLGKKGRVKKAHKSKTH 534
UGT1A1     AKRMETKGAGVTLNVLEMTSEDLENALKAVINDKSYKENIMRLSSLHKDRPVEPLDLAVFWVEFVMRHKGAPHLRPAAHDLTWYQYHSLDVIGFLLAVVLTVAFITFKCCAYGYRKCLGKKGRVKKAHKSKTH 533
UGT1A9     AKRMETKGAGVTLNVLEMTSEDLENALKAVINDKSYKENIMRLSSLHKDRPVEPLDLAVFWVEFVMRHKGAPHLRPAAHDLTWYQYHSLDVIGFLLAVVLTVAFITFKCCAYGYRKCLGKKGRVKKAHKSKTH 530
UGT1A8     AKRMETKGAGVTLNVLEMTSEDLENALKAVINDKSYKENIMRLSSLHKDRPVEPLDLAVFWVEFVMRHKGAPHLRPAAHDLTWYQYHSLDVIGFLLAVVLTVAFITFKCCAYGYRKCLGKKGRVKKAHKSKTH 530
UGT1A7     AKRMETKGAGVTLNVLEMTSEDLENALKAVINDKSYKENIMRLSSLHKDRPVEPLDLAVFWVEFVMRHKGAPHLRPAAHDLTWYQYHSLDVIGFLLAVVLTVAFITFKCCAYGYRKCLGKKGRVKKAHKSKTH 530
UGT1A10    AKRMETKGAGVTLNVLEMTSEDLENALKAVINDKSYKENIMRLSSLHKDRPVEPLDLAVFWVEFVMRHKGAPHLRPAAHDLTWYQYHSLDVIGFLLAVVLTVAFITFKCCAYGYRKCLGKKGRVKKAHKSKTH 530
UGT1A6     AKRMETKGAGVTLNVLEMTSEDLENALKAVINDKSYKENIMRLSSLHKDRPVEPLDLAVFWVEFVMRHKGAPHLRPAAHDLTWYQYHSLDVIGFLLAVVLTVAFITFKCCAYGYRKCLGKKGRVKKAHKSKTH 532
UGT2B7     IAHMKARGAAVRVDFNTMSSTDLLNALKRVINDPSYKENVMKLSRIQHDQPVKPLDRAVFWIEFVMRHKGAKHLRVAAHDLTWFQYHSLDVIGFLLVCVATVIFIVTKCCLFCFWKFA------RKAKKGKND 529
             :*:::**.* ::.  *:* ** **** **** *****:*:** :::*:**:*** ****:********* *** *******:************.  * ** **. *** : : *        :**:*.*..
```

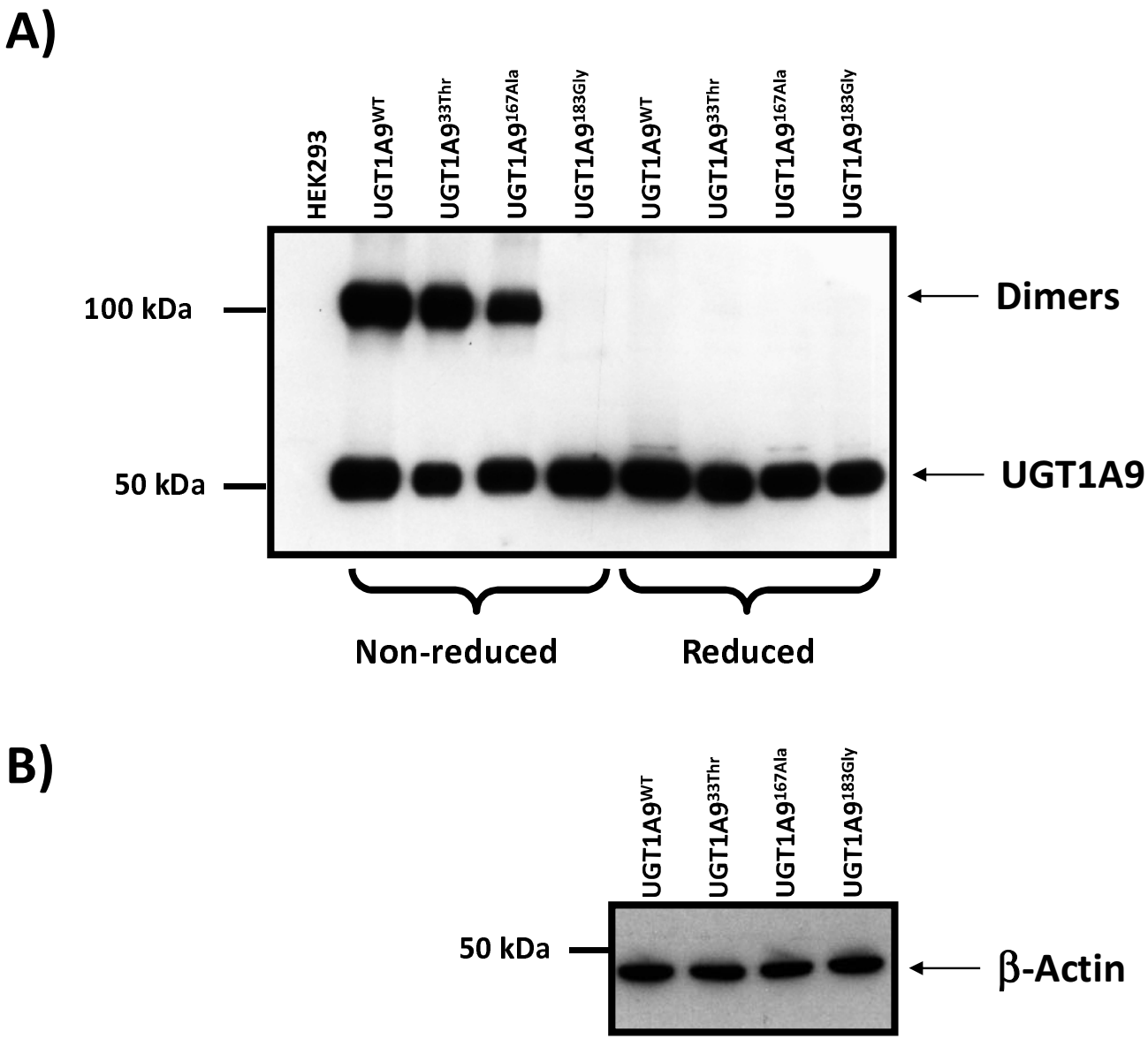

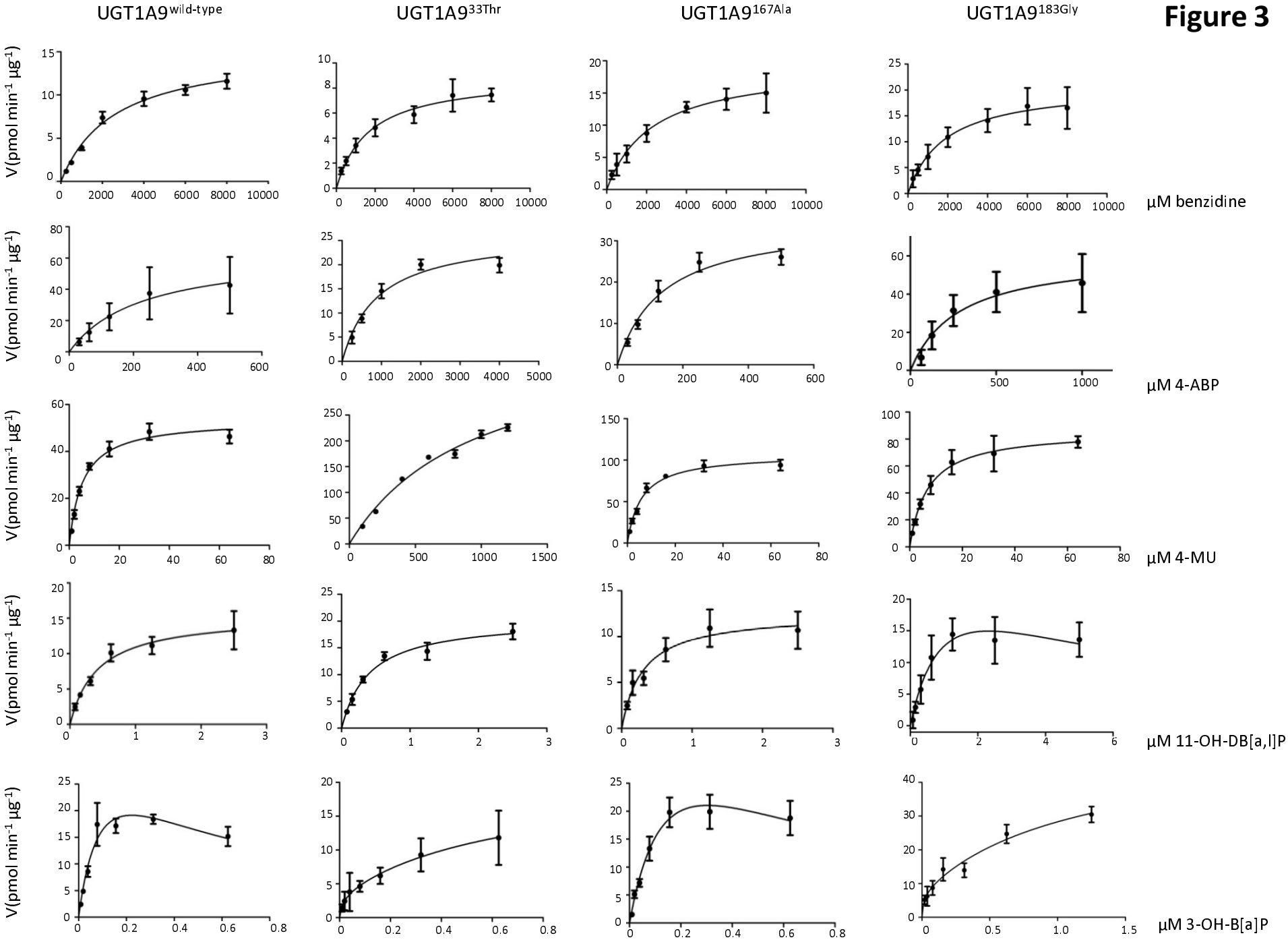

Figure 3

DMD Fast Forward. Published on July 9, 2009 as DOI: 10.1124/dmd.108.024596
This article has not been copyedited and formatted. The final version may differ from this version.

Figure 4